

See discussions, stats, and author profiles for this publication at: <https://www.researchgate.net/publication/49807723>

Ratiometric Fluorescent Chemosensor for Silver Ion at Physiological pH

ARTICLE *in* INORGANIC CHEMISTRY · FEBRUARY 2011

Impact Factor: 4.76 · DOI: 10.1021/ic1018967 · Source: PubMed

CITATIONS

60

READS

26

6 AUTHORS, INCLUDING:



NANDHAKUMAR RAJU

Karunya University

91 PUBLICATIONS 658 CITATIONS

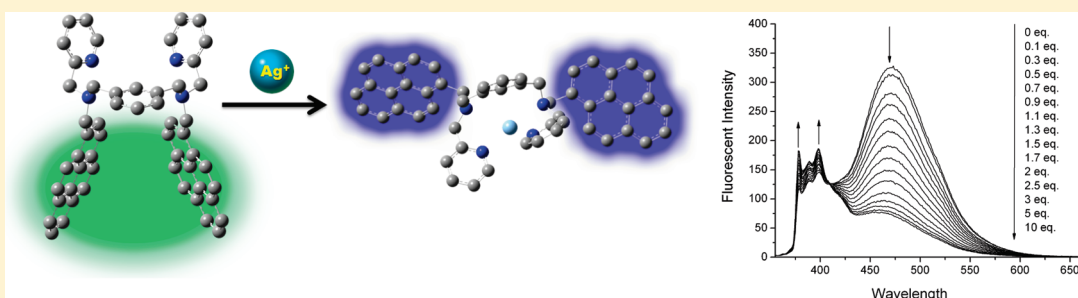
SEE PROFILE

Ratiometric Fluorescent Chemosensor for Silver Ion at Physiological pH

Fang Wang,^{ll,†} Raju Nandhakumar,^{ll,†} Jong Hun Moon,[‡] Kwan Mook Kim,^{*,†} Jin Yong Lee,^{*,‡} and Juyoung Yoon^{*,†,§}[†]Department of Chemistry and Nano Science and [§]Department of Bioinspired Science (WCU), Ewha Womans University, Seoul 120-750, Korea[‡]Department of Chemistry, Sungkyunkwan University, Suwon 440-746, Korea

S Supporting Information

ABSTRACT:



Bis-pyrene derivative **1**, bearing two pyrene and pyridine groups, was synthesized as a ratiometric fluorescent chemosensor for Ag^+ in aqueous solution. Fluorescent chemosensor **1** displayed a selective ratiometric change with Ag^+ , which was attributed to the excimer–monomer emissions of pyrenes. A mechanism for the binding mode was proposed based on fluorescence changes, NMR experiments, and theoretical calculations.

INTRODUCTION

Ag^+ is widely used in the electrical industry, photography/imaging industry, and pharmaceutical industry.^{1,2} Because of the high toxicity of Ag^+ in aquatic organisms, monitoring of Ag^+ levels has been an important issue. Additionally, it is known that silver can inactivate sulphhydryl enzymes and accumulate in the body.² Even though a few Ag^+ detection methods such as inductively coupled plasma mass spectrometry (ICP-MS),³ atomic absorption spectrometry,⁴ and others are currently used, they suffer from being costly and time-consuming processes. Accordingly, a simple method for detecting Ag^+ is needed.

Sensors based on the ion-induced changes in fluorescence have been actively investigated because of their simplicity and high detection limit for fluorescence.⁵ A few fluorescent chemosensors based on small molecules have been reported which can detect Ag^+ in organic solvent⁶ and aqueous solution;⁷ however, to our knowledge, there has been only one example of a ratiometric fluorescent sensor for Ag^+ which works in aqueous solution.^{7d} Ratiometric fluorescent sensors have a few advantages. The ratio between the two emission intensities can be used to evaluate the analyte concentration and provide a built-in correction for environmental effects, such as photobleaching, sensor molecule concentration, the environment around the sensor molecule (pH, polarity, temperature, etc.), and stability under illumination.^{8,9} In addition, oligonucleotides¹⁰ and quantum dots¹¹ were also recently utilized as ensembles of Ag^+ selective sensors.

We report herein a new bis-pyrene derivative bearing two pyridine groups as a selective fluorescent sensor for Ag^+ . Among the various metal ions examined, probe **1** displays a selective and unique ratiometric fluorescence change with Ag^+ at pH 7.4, which was attributed to the excimer–monomer emissions of pyrenes. The mechanism for the binding mode was proposed based on fluorescence changes, NMR experiments, and theoretical calculations.

EXPERIMENTAL SECTION

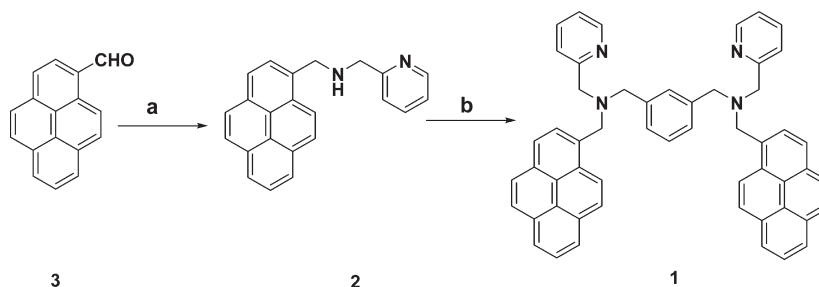
General methods unless otherwise noted; materials were obtained from commercial suppliers and were used without further purification. Flash chromatography was carried out on silica gel (230–400 mesh). ¹H NMR and ¹³C NMR spectra were recorded using 250 and 62.9 MHz. Chemical shifts were expressed in parts per million (ppm) and coupling constants (*J*) in hertz (Hz).

Preparation of Fluorometric Titration Solutions. Stock solutions (0.01 M) of the perchlorate salts (or chloride salts) of Ag^+ , Al^{3+} , Ca^{2+} , Cd^{2+} , Co^{2+} , Cu^{2+} , Fe^{2+} , Fe^{3+} , Hg^{2+} , K^+ , Li^+ , Mg^{2+} , Mn^{2+} , Na^+ , Ni^{2+} , Pb^{2+} , Sr^{2+} , and Zn^{2+} in water were prepared. Stock solutions of host (1 mM) were prepared in DMSO/HEPES (0.02 M, pH 7.4) (1:1). Test solutions were prepared by placing 100 μL of the probe stock solution into a test tube, adding an appropriate aliquot of each ion's

Received: September 16, 2010

Published: February 03, 2011

Scheme 1. Synthesis of Compound 1 and 2



^a i. pyridine-2-methylamine, EtOH/CHCl₃, reflux, 3 h, ii. EtOH, NaBH₄, 3 h, rt. ^b *m*-Xylene dibromide, K₂CO₃, CH₃CN, reflux, 12 h.

stock, and diluting the solution to 10 mL with DMSO/HEPES (0.02 M, pH 7.4) (1:1). For all measurements, excitation and emission slit widths were 3 nm.

Compound 2 [*N*-((pyren-3-yl) methyl) (pyridin-2-yl) methanamine]. Pyrene carboxaldehyde (1 g, 4.4 mmol) and pyridine-2-methylamine (0.52 g, 4.8 mmol) were dissolved in a co-solvent of absolute ethanol (30 mL) and chloroform (5 mL). The mixture was degassed with nitrogen and then heated under reflux for 3 h. After being cooled to room temperature, the precipitate was separated and washed with ethanol (ice cold) to afford the crude Schiff base. The Schiff base was combined with NaBH₄ (0.17 g, 4.4 mmol) and ethanol (30 mL). The resulting reaction mixture was stirred at room temperature for 3 h. The solvent was then removed, and methylene chloride (30 mL) and HCl (0.2 N, 30 mL) were added. After being stirred for 1 h, the organic layer was separated and washed with 0.5 N NaOH aqueous solution, water, brine, and dried over MgSO₄. After removal of the solvent, the residue was passed through a short silica gel column, and eluted with ethylacetate/methanol (10:1) to afford the desired oily product 2. Yield: 1.15 g (82%). ¹H NMR (CDCl₃, 250 MHz): δ (ppm): 8.61 (d, 1H, *J* = 4.79 Hz, C₆H₄N), 8.35 (d, 1H, *J* = 9.26 Hz, pyrene-H), 8.18–7.98 (m, 8H, pyrene-H), 7.59 (t, 1H, *J* = 7.40 Hz, C₆H₄N), 7.31 (d, 1H, *J* = 7.73 Hz, C₆H₄N), 7.15 (t, 1H, *J* = 6.17 Hz, C₆H₄N), 4.52 (s, 2H), 4.09 (s, 2H), 2.46 (s, 1H). ¹³C NMR (CDCl₃, 62.9 MHz): δ (ppm): 51.33, 54.62, 55.05, 55.45, 76.68, 77.19, 77.39, 77.69, 121.98, 122.42, 123.32, 124.69, 124.98, 125.01, 125.04, 125.84, 127.05, 127.09, 127.47, 127.55, 129.17, 130.68, 130.86, 131.32, 133.68, 136.43, 148.86, 149.30, 149.73, 159.86. FAB-MS *m/z* = 323.16 (M+H)⁺, calcd for C₂₃H₁₈N₂ = 322.15.

Compound 1. Compound 2 (0.7 g, 2.2 mmol), K₂CO₃ (0.4 g, 3 mmol), and dry CH₃CN (10 mL) were placed in a round-bottom flask under a N₂ atmosphere at room temperature. To this mixture, a CH₃CN solution (40 mL) of *m*-xylene dibromide (0.26 g, 1.0 mmol) was added dropwise under N₂ atmosphere over 30 min. The reaction mixture was then heated to reflux for 12 h. After being cooled to room temperature, the insoluble materials were removed by filtration, and washed with chloroform several times until the washing solvent became colorless. The combined filtrate was concentrated, and the resulting residue was purified by silica gel column chromatography by using ethyl acetate/hexanes (1:1) as an eluent to give the final sensor 1. Yield: 0.45 g (60%) Mp: 92 °C. ¹H NMR (CDCl₃, 250 MHz): δ (ppm): 8.48 (d, 2H, *J* = 4.72 Hz), 8.30 (d, 2H, *J* = 9.28 Hz), 8.15–7.89 (m, 16H, pyrene-H), 7.60 (s, 1H), 7.46–7.45 (m, 4H), 7.33 (s, 3H), 7.02 (d, 2H, *J* = 4.86 Hz), 4.31 (s, 4H), 3.86 (s, 4H), 3.76 (s, 4H). ¹³C NMR (CDCl₃, 62.9 MHz): δ (ppm): 56.88, 59.20, 60.19, 121.85, 123.08, 123.97, 124.42, 124.68, 124.89, 125.76, 126.93, 127.36, 128.07, 128.17, 129.75, 130.64, 131.22, 132.66, 136.29, 139.10, 148.57, and 160.06. FAB-MS *m/z* = 747.35 (M+H)⁺, calcd for C₅₄H₄₂N₄ = 746.34.

Calculation Methods. To investigate the interaction mode and to understand the fluorescence behavior of 1 in the presence of Ag⁺ ion, we

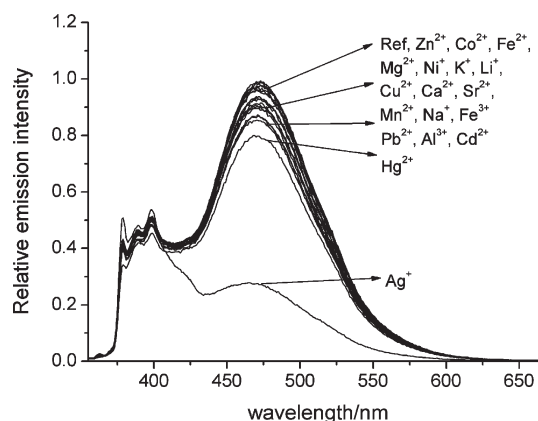


Figure 1. Fluorescence changes of 1 (10 μ M) with various metal ions (20 μ M) in DMSO-HEPES (pH 7.4, 1:1, v/v). (λ_{ex} = 344 nm, Slit: 3 nm/5 nm).

carried out density functional theory (DFT) calculations with Becke's three parametrized Lee–Yang–Parr (B3LYP)¹² exchange functional with 6-31G* basis sets, using a suite of Gaussian 03 programs.¹³ The 6-31G* calculations for 1 and 1·Ag⁺ complexes were performed except for Ag⁺, where the LANL2DZpd¹⁴ effective core potential (ECP) was utilized.

RESULTS AND DISCUSSION

Synthesis. For the synthesis of probe 1, intermediate product 2 was synthesized in 82% yield from pyrene carboxaldehyde and pyridine-2-methylamine, followed by sodium borohydride reduction (Scheme 1). Treatment of intermediate 2 with *m*-xylene dibromide gave probe 1 in 60% yield after purification by silica gel column chromatography, using ethyl acetate/hexanes (1:1) as an eluent. These new compounds were fully characterized by NMR and high resolution FAB mass spectroscopy. The ¹H NMR, ¹³C NMR, and FAB mass spectra were reported in the Supporting Information (Figures S1–S5).

Fluorescence Experiments. Ag⁺, Al³⁺, Ca²⁺, Cd²⁺, Co²⁺, Cu²⁺, Fe²⁺, Fe³⁺, Hg²⁺, K⁺, Li⁺, Mg²⁺, Mn²⁺, Na⁺, Ni²⁺, Pb²⁺, Sr²⁺, and Zn²⁺ ions were used to evaluate the metal ion binding properties of the probe (10 μ M) in DMSO-HEPES (pH 7.4, 1:1, v/v). The fluorescence spectra were obtained by excitation of the pyrene fluorophore at 344 nm (Figure 1). In the absence of metal ions, a strong excimer peak was observed at 463 nm along with a monomeric peak at 399 nm, which means there is a strong π – π interaction between the two pyrene moieties of probe 1 in aqueous solution. Among these metal ions (20 μ M),

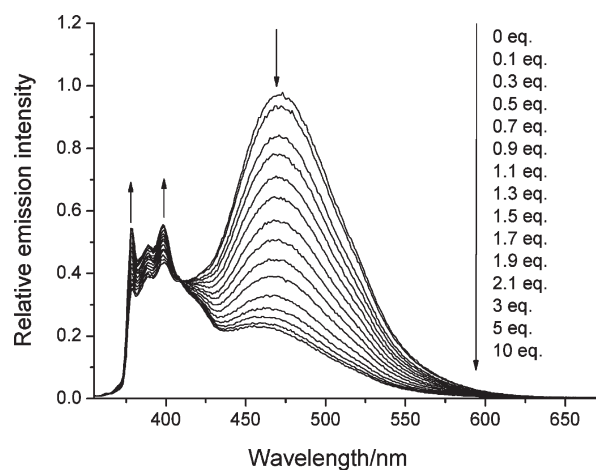


Figure 2. Fluorescence titrations of **1** (10 μ M) with Ag^+ in DMSO-HEPES (pH 7.4, 1:1, v/v) (λ_{ex} = 344 nm, Slit: 3 nm/5 nm).

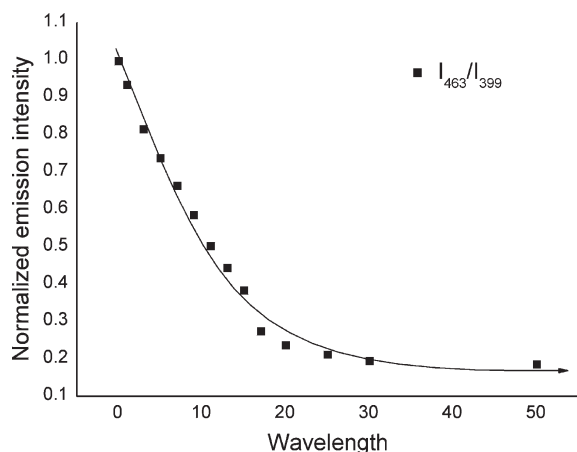


Figure 3. Ratio of fluorescence at 463 nm and at 399 nm as a function of Ag^+ concentration.

probe **1** showed a selective fluorescence change only with Ag^+ , even though there was a relatively smaller quenching effect with Hg^{2+} . Common quenchers, such as Co^{2+} , Fe^{3+} , Cu^{2+} , and Mn^{2+} , surprisingly did not show significant quenching effects.

Figure 2 shows the fluorescence titrations of **1** with Ag^+ in DMSO-HEPES (pH 7.4, 1:1, v/v). An excimer peak was significantly reduced, with the enhancement of a monomeric peak upon the addition of Ag^+ . The ratiometric changes at 463 and 399 nm were displayed in Figure 3. The association constant of **1** with Ag^+ was calculated as $3.2 \times 10^5 \text{ M}^{-1}$ (error < 15%).¹⁵ The 1:1 stoichiometry was confirmed by Electrospray Ionization (ESI) mass spectroscopy and Job plots, as shown in the Supporting Information (Figures S6 and S7). A peak at m/z 853.5, which corresponds to $[\text{Ag}(\textbf{1})]^+$, was clearly observed in the ESI mass spectrum. The ratiometric calibration curve (I_{463}/I_{399}), as a function of Ag^+ concentration, is valid up to the presence of 5 equiv of Ag^+ (Figure 3). The ratiometric changes of sensor **1** at 463 and 399 nm are proportional to the addition of Ag^+ at concentrations of 0–20 μ M. In addition, similar fluorescence changes with Ag^+ were observed between pH 6.8 and 8.2 (Supporting Information, Figure S8). The fluorescence changes of **1** with 5 equiv of various metal ions and UV absorption change of **1** in the presence of Ag^+ are shown in the Supporting Information

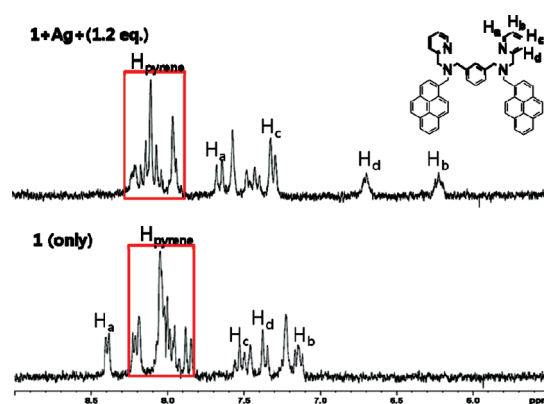


Figure 4. Partial ^1H NMR spectra (250 MHz) of probe **1** upon the addition of silver perchlorate (1.2 equiv) in DMSO- d_6 - D_2O (8:2, v/v).

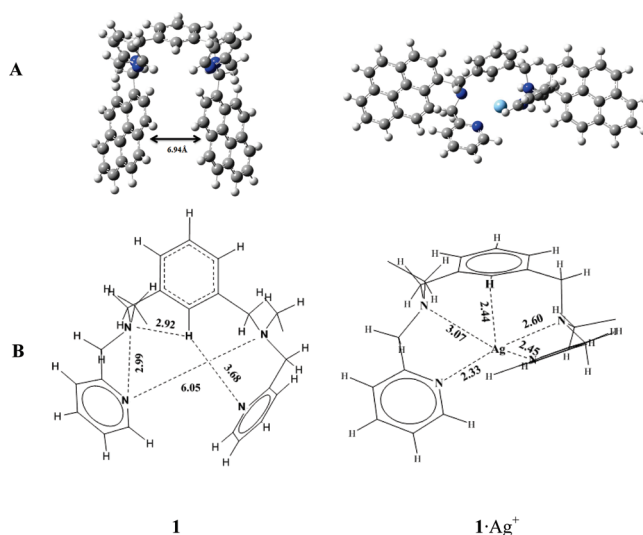


Figure 5. Calculated structures (A) and exaggerated drawing to give the binding mode (B) between **1** and Ag^+ .

(Figure S9 and Figure S10, respectively). On the other hand, Hg^{2+} showed fluorescence quenching effects both for monomer and for excimer emissions as shown in the Supporting Information (Figure S11). From the fluorescence titrations of **1** with Hg^{2+} (Supporting Information, Figure S11) in DMSO-HEPES (pH 7.4 1:1, v/v), the association constant of **1** with Hg^{2+} was calculated as $1.0 \times 10^4 \text{ M}^{-1}$ (error < 20%).¹⁵ Fluorescence spectral change of intermediate **2** with Ag^+ is shown in the Supporting Information (Figure S12). There is no intermolecular excimer formation of intermediate **2** in the presence of Ag^+ .

NMR Experiments. The binding of **1** with Ag^+ was further confirmed by ^1H NMR spectra (Figure 4). When 1 equiv of Ag^+ was added to **1** in DMSO- d_6 - D_2O (8:2, v/v), shielding effects were observed as shown in Figure 4. On the basis of the 2D COSY NMR spectra (Supporting Information, Figures S13 and S14), protons on pyridine rings could be assigned. Large upfield shifts were especially observed for protons on pyridine rings as shown in Figure 4. For example, H_a moves from δ 8.39 ppm to 7.64 ppm ($\Delta\delta$ = 0.75) and the shifts ($\Delta\delta$) for H_b , H_c , and H_d are 0.92 (from δ 7.15 ppm to 6.23 ppm), 0.25 (from δ 7.53 ppm to 7.28 ppm), and 0.67 (from δ 7.38 ppm to 6.71 ppm), respectively. These large upfield shifts especially for H_a , H_b , and H_d can be attributed to the close proximity of pyridine and phenyl groups

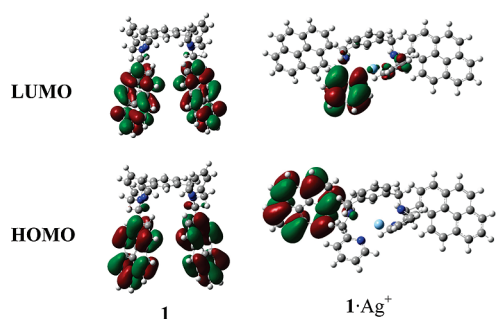


Figure 6. Calculated HOMO and LUMO of **1** and **1**·Ag⁺.

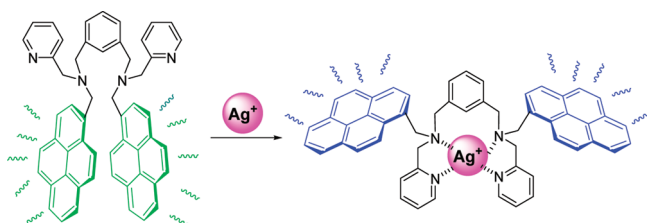


Figure 7. Schematic fluorescence origin of **1** (excimer emission) and **1**·Ag⁺ (monomer emission).

upon the addition of Ag⁺, which was also confirmed by theoretical calculations. ¹H NMR titration spectra are also explained in the Supporting Information (Figure S15).

Theoretical Calculations. To investigate the interaction mode and to understand the fluorescence behavior of **1** in the presence of Ag⁺ ion, we carried out density functional theory (DFT) calculations with Becke's three parametrized Lee–Yang–Parr (B3LYP)¹² exchange functional with 6-31G* basis sets, using a suite of Gaussian 03 programs.¹³ The 6-31G* calculations for **1** and **1**·Ag⁺ complexes were performed except for Ag⁺, where the LANL2DZpd effective core potential (ECP)¹⁴ was utilized. The optimized structures of **1** and **1**·Ag⁺ are shown in Figure 5(A). Compound **1** has well stacked pyrenes with an interpyrene distance of 6.94 Å and a N···N interatomic distance of 6.05 Å, where the two pyrenes are quite far but may form an excimer without difficulty by excitation. For **1**·Ag⁺, we tested several possible binding modes, showing either Ag⁺···pyrene or Ag⁺···N interaction. Among them, the Ag⁺···N interaction type structure was much more stable than the pyrene···Ag⁺···pyrene type structure (having cation···π interactions). As noted in Figure 5(B), in the Ag⁺···N interaction type structure, Ag⁺ was coordinated by four nitrogen atoms, where the distances between Ag⁺ and nitrogen atoms were about 2.58 Å, and the interaction energy was calculated to be −72.86 kcal/mol. Following the addition of Ag⁺, the N···N interatomic distance decreased from 6.05 Å to 5.05 Å.

To understand the origin of the changes in the chemical shift of **1** with the presence of Ag⁺ in the NMR experiment, we simulated the ¹H NMR spectra of **1** and **1**·Ag⁺, and the results are shown in the Supporting Information (Figure S16). The simulated spectra were obtained in the gas phase. Nevertheless, the simulated ¹H NMR spectra are qualitatively in good agreement with the experiment, thus, the binding mode presented in Figure 5 seems to be acceptable because the ¹H NMR spectra are highly dependent on the conformational changes; that is, the shielding and deshielding regions are severely affected and changed by the conformational changes. In the experiment, the calculated

chemical shifts of the pyridinyl protons of **1** were consistently upfield, while the pyrene protons were somewhat downfield shifted upon addition of Ag⁺. It was found from the calculated structures, that the upfield shift of the pyridinyl protons mainly arise from the fact that they are positioned in a more shielded region under the influence of the central phenyl ring, as shown in Figure 5.

In addition, the chemical shifts of the methylene protons (next to the pyridinyls) were calculated to be 2.32 and 3.73 ppm in **1**, while they were slightly downfield shifted to 2.67, 3.06, 4.14, and 4.15 ppm in **1**·Ag⁺. Similarly, the methylene protons next to the pyrenes were also downfield shifted from 3.45 and 3.63 ppm in **1** to 4.31, 4.90, 4.99, and 5.45 ppm in **1**·Ag⁺. The downfield shift was found to originate from the electron withdrawing nature of Ag⁺, which made the nitrogen atoms sandwiched by two methylene groups electron deficient, as confirmed by the atomic charges obtained from the natural bond orbital (NBO) population analysis.

To further understand the fluorescence behavior of **1** and **1**·Ag⁺, time-dependent density functional theory (TDDFT) calculations were performed at the optimized geometries. The main transition property of **1** was determined that the HOMO to LUMO+1 and HOMO-1 to LUMO transitions predominantly contribute to the electronic excitations with 90% contribution. In **1**·Ag⁺ complex, the main transition comes from HOMO to LUMO+3 and HOMO to LUMO+4 with 85% contribution. More detailed information for the contributions of orbital transitions for some electronic transitions with large oscillator strengths see the Supporting Information (Tables S1 and S2).

Figure 6 represents the highest occupied molecular orbital (HOMO) and the lowest unoccupied molecular orbital (LUMO) of **1** and **1**·Ag⁺. The other relevant frontier molecular orbitals are given in the Supporting Information, Figure S17. It can be noted that the excited state (LUMO) of the two pyrene units shows a strong interaction between the two pyrene moieties in **1**. However, the **1**·Ag⁺ complex does not show such interactions between pyrene moieties because of the intramolecular charge transfer from the pyrene to the nearby pyridine and Ag⁺ ions, as seen in LUMO, LUMO+1, LUMO+3, and LUMO+4. It can be inferred from the LUMOs that, in the excited state, the two pyrene units show a strong interaction between the two pyrene moieties in **1**; however in the **1**·Ag⁺ complex such interactions between pyrene moieties could not be possible because of the intramolecular charge transfer from the pyrene to the nearby pyridine and Ag⁺ ions. Therefore, the excimer emission was dramatically quenched and only the monomer emission existed in **1**·Ag⁺. On the basis of the calculation results, the binding mode is proposed in Figure 7.

CONCLUSION

We report a new bis-pyrene probe containing two pyridine groups as a selective and ratiometric sensor for Ag⁺ at pH 7.4. Upon the addition of Ag⁺, differences in excimer and monomer emissions induce significant ratiometric changes. The previous ratiometric sensor containing one pyrene group showed 1:2 binding with Ag⁺;^{7d} on the other hand, **1** displayed 1:1 binding mode. Comparing the calculated structure and NMR spectra with the NMR experiment, a reasonable binding mode between **1** and Ag⁺ is proposed, and the fluorescence behavior is explained based on the molecular orbital shapes and excitation properties obtained from TDDFT calculations. We believe this approach

for a ratiometric sensor can be applied to other analytes by modifying the ligand system.

■ ASSOCIATED CONTENT

S Supporting Information. Job plot, UV data, ^1H NMR and ^{13}C NMR of probe **1**, ESI mass spectrum of $[\text{1}(\text{Ag})]^+$ and ^1H NMR titration spectra, and calculated structures of **1** and $\text{1} \cdot \text{Ag}^+$. This material is available free of charge via the Internet at <http://pubs.acs.org>.

■ AUTHOR INFORMATION

Corresponding Author

*E-mail: kkmoock@ewha.ac.kr (K.M.K.), jinyilee@skku.edu (J.Y.L.), jyoon@ewha.ac.kr (J.Y.).

Author Contributions

^{||} Contributed equally to this work.

■ ACKNOWLEDGMENT

J.Y. acknowledges National Research Foundation of Korea (NRF) (2010-0018895, 2010-0001481) and WCU (R31-2008-000-10010-0) program. K.M.K. acknowledges NRF (2010-0008022, 2010-0001482) and R.N. acknowledges RP-Grant 2010 of Ewha Womans University. The work at SKKU was supported by the NRF grant (NO. 20100001630) and Samsung Research Fund, Sungkyunkwan University, 2010. Mass spectral data were obtained from the Korea Basic Science Institute (Daegu) on a Jeol JMS 700 high resolution mass spectrometer.

■ REFERENCES

- (1) Barriada, J. L.; Tappin, A. D.; Evans, E. H.; Achterberg, E. P. *TrAC, Trends Anal. Chem.* **2007**, *26*, 809.
- (2) Ratte, H. T. *Environ. Toxicol. Chem.* **1999**, *18*, 89.
- (3) Karunasagar, D.; Arunachalam, J.; Gangadharan, S. J. *Anal. At. Spectrom.* **1998**, *13*, 679.
- (4) Li, Y.; Chen, C.; Li, B.; Sun, J.; Wang, J.; Gao, Y.; Zhao, Y.; Chai, Z. *J. Anal. At. Spectrom.* **2006**, *21*, 94.
- (5) (a) Czarnik, A. W. *Acc. Chem. Res.* **1994**, *27*, 302; (b) de Silva, A. P.; Gunaratne, H. Q. N.; Gunnlaugsson, T. A.; Huxley, T. M.; McCoy, C. P.; Rademacher, J. T.; Rice, T. E. *Chem. Rev.* **1997**, *97*, 1515; (c) Gunnlaugsson, T.; Glynn, M.; Tocchi, G. M.; Kruger, P. E.; Pfeffer, F. M. *Coord. Chem. Rev.* **2006**, *250*, 3094; (d) Kim, J. S.; Quang, D. T. *Chem. Rev.* **2007**, *107*, 3780; (e) Xu, Z.; Chen, X.; Kim, H. N.; Yoon, J. **2010**, *39*, 127. (f) Chen, X.; Zhou, Y.; Peng, X.; Yoon, J. *Chem. Soc. Rev.* **2010**, *39*, 2120. (g) Xu, Z.; Kim, S. K.; Yoon, J. *Chem. Soc. Rev.* **2010**, *39*, 1457. (h) Kim, H. N.; Guo, Z.; Zhu, W.; Yoon, J.; Tian, H. *Chem. Soc. Rev.* **2011**, *40*, 79. (i) Chen, X.; Kang, S.; Kim, M. J.; Kim, J.; Kim, Y. S.; Kim, H.; Chi, B.; Kim, S.-J.; Lee, J. Y.; Yoon, J. *Angew. Chem., Int. Ed.* **2010**, *49*, 1422. (j) Xu, Z.; Baek, K.-H.; Kim, H. N.; Cui, J.; Qian, X.; Spring, D. R.; Shin, J.; Yoon, J. *J. Am. Chem. Soc.* **2010**, *132*, 601.
- (6) (a) Kang, J.; Choi, M.; Lee, E. Y.; Yoon, J. *J. Org. Chem.* **2002**, *67*, 4384. (b) Coskun, A.; Akkaya, E. U. *J. Am. Chem. Soc.* **2005**, *127*, 10464. (c) Shamsipur, M.; Alizadeh, K.; Hosseini, M.; Caltagirone, C.; Lippolis, V. *Sens. Actuators B* **2006**, *113*, 892. (d) Tong, H.; Wang, L. X.; Ting, X. B.; Wang, F. *Macromolecules* **2002**, *35*, 7169. (e) Parker, J.; Glass, T. E. *J. Org. Chem.* **2001**, *66*, 6505. (f) Ishikawa, J.; Sakamoto, H.; Nakao, S.; Wada, H. *J. Org. Chem.* **1999**, *64*, 1913. (g) Huang, C.; Peng, X.; Lin, Z.; Fan, J.; Ren, A.; Sun, D. *Sens. Actuators B* **2008**, *133*, 113. (h) Kim, S. K.; Lee, J. K.; Lee, S. H.; Lim, M. S.; Lee, S. W.; Sim, W.; Kim, J. S. *J. Org. Chem.* **2004**, *69*, 2877. (i) Kim, J. S.; Yang, S. H.; Rim, J. A.; Kim, J. Y.; Vicens, J.; Shinkai, S. *Tetrahedron Lett.* **2001**, *42*, 8047. (j) Lin, H.; Cinar, M. E.; Schmittell, M. *Dalton Trans.* **2010**, *39*, 5130. (k) Ray, D.; Iyer, E.; Siva, S.; Sadhu, K. K.; Bharadwaj, P. K. *Dalton Trans.* **2009**, 5683. (l) Hung, H.-C.; Cheng, C.-W.; Wang, Y.-Y.; Chen, Y.-J.; Chung, W.-S. *Eur. J. Org. Chem.* **2009**, 6360. (m) Joseph, R.; Ramanujam, B.; Acharya, A.; Rao, C. P. *J. Org. Chem.* **2009**, *74*, 8181. (n) Liu, L.; Zhang, D.; Zhang, G.; Xiang, J.; Zhu, D. *Org. Lett.* **2008**, *10*, 2271. (o) Rurack, K.; Kollmannsberger, M.; Resch-Genger, U.; Daub, J. *J. Am. Chem. Soc.* **2000**, *122*, 968. (p) Kandaz, M.; Güney, O.; Senkal, F. B. *Polyhedron* **2009**, *28*, 3110. (q) Wang, H.-H.; Xue, L.; Qian, Y.-Y.; Jiang, H. *Org. Lett.* **2010**, *12*, 292.
- (7) (a) Swamy, K. M. K.; Kim, H. N.; Soh, J. H.; Kim, Y.; Kim, S.-J.; Yoon, J. *Chem. Commun.* **2009**, 1234. (b) Chatterjee, A.; Santra, M.; Won, N.; Kim, S.; Kim, J. K.; Kim, S. B.; Ahn, K. H. *J. Am. Chem. Soc.* **2009**, *131*, 2040. (c) Lin, C.-Y.; Yu, C.-J.; Lin, Y.-H.; Tseng, W.-L. *Anal. Chem.* **2010**, *82*, 6830. (d) Yang, R.-H.; Chan, W.-H.; Lee, A. W. M.; Xia, P.-F.; Zhang, H.-K.; Li, K. A. J. *Am. Chem. Soc.* **2003**, *125*, 2884. (e) Lyoshi, S.; Taki, M.; Yamamoto, Y. *Inorg. Chem.* **2008**, *47*, 3946. (f) Park, C. S.; Lee, J. Y.; Kang, E.-J.; Lee, J.-E.; Lee, S. S. *Tetrahedron Lett.* **2009**, *50*, 671. (g) Schmittell, M.; Lin, H. *Inorg. Chem.* **2007**, *46*, 9139. (h) Xu, Z.; Zheng, S.; Yoon, J.; Spring, D. R. *Analyst* **2010**, *135*, 2554.
- (8) Grynkiewicz, G.; Poenie, M.; Tsien, R. Y. *J. Biol. Chem.* **1985**, *260*, 3440.
- (9) (a) Xu, Z.; Qian, X.; Cui, J. *Org. Lett.* **2005**, *7*, 3029. (b) Xu, Z.; Singh, N. J.; Lim, J.; Pan, J.; Kim, H. N.; Park, S.; Kim, K. S.; Yoon, J. *J. Am. Chem. Soc.* **2009**, *131*, 15528. (c) Xu, Z.; Kim, S. K.; Han, S. J.; Lee, C.; Kociok-Kohn, G.; James, T. D.; Yoon, J. *Eur. J. Org. Chem.* **2009**, *18*, 3058. (d) Parab, K.; Venkatasubbiah, K.; Jakle, F. J. *Am. Chem. Soc.* **2006**, *128*, 12879. (e) Maruyama, S.; Kikuchi, K.; Hirano, T.; Urano, Y.; Nagano, T. *J. Am. Chem. Soc.* **2002**, *124*, 10650. (f) Zhou, G.; Baumgarten, M.; Mulle, K. J. *Am. Chem. Soc.* **2008**, *130*, 12477. (g) Zhou, Y.; Fang, W.; Kim, Y.; Kim, S.; Yoon, J. *Org. Lett.* **2009**, *11*, 4442. (h) Zhang, J. F.; Zhou, Y.; Yoon, J.; Kim, Y.; Kim, S. J.; Kim, J. S. *Org. Lett.* **2010**, *12*, 3852.
- (10) (a) Wen, Y.; Xing, F.; He, S.; Song, S.; Wang, L.; Long, Y.; Li, D.; Fan, C. *Comm. Commun.* **2010**, *46*, 259. (b) Lin, Y.-H.; Tseng, W.-L. *Comm. Commun.* **2009**, 6619. (c) Li, T.; Shi, L.; Wang, E.; Dong, S. *Chem.—Eur. J.* **2009**, *15*, 3347. (d) Ono, A.; Cao, S.; Togashi, H.; Tashiro, M.; Fujimoto, T.; Machinami, T.; Oda, S.; Miyake, Y.; Okamoto, I.; Tanaka, Y. *Comm. Commun.* **2008**, 4825.
- (11) (a) Zhang, B.-H.; Qi, L.; Wu, F.-Y. *Microchim. Acta* **2010**, *170*, 147. (b) Lin, C.-Y.; Yu, C.-J.; Lin, Y.-H.; Tseng, W.-L. *Anal. Chem.* **2010**, *82*, 6831. (c) Freeman, R.; Finder, T.; Willner, I. *Angew. Chem., Int. Ed.* **2009**, *48*, 7818. (d) Li, B.; Du, Y.; Dong, S. *Anal. Chim. Acta* **2009**, *644*, 78. (e) Gattás-Asfura, K. M.; Leblanc, R. M. *Comm. Commun.* **2003**, 2684.
- (12) (a) Becke, A. D. *J. Chem. Phys.* **1993**, *98*, 5648. (b) Lee, C.; Yang, W.; Parr, R. G. *Phys. Rev. B* **1988**, *37*, 785.
- (13) Frisch, M. J.; Trucks, G. W.; Schlegel, H. B.; Scuseria, G. E.; Robb, M. A.; Cheeseman, J. R.; Montgomery, Jr., J. A.; Vreven, T.; Kudin, K. N.; Burant, J. C.; Millam, J. M.; Iyengar, S. S.; Tomasi, J.; Barone, V.; Mennucci, B.; Cossi, M.; Scalmani, G.; Rega, N.; Petersson, G. A.; Nakatsuji, H.; Hada, M.; Ehara, M.; Toyota, K.; Fukuda, R.; Hasegawa, J.; Ishida, M.; Nakajima, T.; Honda, Y.; Kitao, O.; Nakai, H.; Klene, M.; Li, X.; Knox, J. E.; Hratchian, H. P.; Cross, J. B.; Bakken, V.; Adamo, C.; Jaramillo, J.; Gomperts, R.; Stratmann, R. E.; Yazyev, O.; Austin, A. J.; Cammi, R.; Pomelli, C.; Ochterski, J. W.; Ayala, P. Y.; Morokuma, K.; Voth, G. A.; Salvador, P.; Dannenberg, J. J.; Zakrzewski, V. G.; Dapprich, S.; Daniels, A. D.; Strain, M. C.; Farkas, O.; Malick, D. K.; Rabuck, A. D.; Raghavachari, K.; Foresman, J. B.; Ortiz, J. V.; Cui, Q.; Baboul, A. G.; Clifford, S.; Cioslowski, J.; Stefanov, B. B.; Liu, G.; Liashenko, A.; Piskorz, P.; Komaromi, I.; Martin, R. L.; Fox, D. J.; Keith, T.; Al-Laham, M. A.; Peng, C. Y.; Nanayakkara, A.; Challacombe, M.; Gill, P. M. W.; Johnson, B.; Chen, W.; Wong, M. W.; Gonzalez, C.; and Pople, J. A. *Gaussian 03*, Revision D.02; Gaussian Inc.; Pittsburg, PA, 2006.

(14) (a) Hay, P. J.; Wadt, W. R. *J. Chem. Phys.* **1985**, 82, 270. (b) Hay, P. J.; Wadt, W. R. *J. Chem. Phys.* **1985**, 82, 284. (c) Hay, P. J.; Wadt, W. R. *J. Chem. Phys.* **1985**, 82, 299.

(15) (a) Association constants were obtained using the computer program ENZFITTER, available from Elsevier-BIOSOFT, 68 Hills Road, Cambridge CB2 1LA, United Kingdom. (b) Connors, K. A. *Binding Constants, The Measurement of Molecular Complex Stability*; Wiley: New York, 1987.